



Time Dependent Deformations in Squeezing Tunnels

Giovanni Barla, Professor of Rock Mechanics, Department of Structural and Geotechnical Engineering, Politecnico di Torino, Italy; e-mail: giovanni.barla@polito.it

Mariacristina Bonini, Research Associate, Department of Structural and Geotechnical Engineering, Politecnico di Torino, Italy; e-mail: mariacristina.bonini@polito.it

Daniele Debernardi, Research Associate, Department of Structural and Geotechnical Engineering, Politecnico di Torino, Italy; e-mail: daniele.debernardi@polito.it

ABSTRACT: *This paper deals with full face excavation of large size tunnels in rock masses of very poor quality which exhibit squeezing problems. Three different time dependent constitutive models of increasing complexity (a viscoelastic-plastic model, an elastic-viscoplastic model, and an elastic-plastic-viscoplastic model) are used to analyze the tunnel response during excavation of the Saint Martin La Porte access adit, along the Lyon-Turin Base Tunnel. The interest of the paper stems from the innovative excavation-construction method adopted and the use of yielding support elements incorporated in the primary lining in order to cope with the squeezing problems encountered in crossing a Carboniferous Formation, a highly heterogeneous, disrupted and fractured rock mass, which is often affected by faulting. The tunnel response is back-analysed by using a semi-analytical solution and finite difference modelling in plane strain and axisymmetric conditions when accounting for the time dependent behaviour of the rock mass. The results of modelling are compared with convergence monitoring data and strain distributions measured around the tunnel. The aim is to highlight advantages and disadvantages of different time dependent constitutive models in reproducing the observed tunnel behaviour in both short term and long term conditions. The information provided is of relevance in relation to modelling the tunnel response in severe to extreme squeezing conditions, with acceptable level of confidence, and to the need to optimize in such conditions the type of support adopted and the excavation/support sequence implemented during face advance.*

KEYWORDS: Tunnelling, monitoring, squeezing, time dependent behaviour, numerical modelling

SITE LOCATION: [IJGCH-database.kmz](#) (requires Google Earth)

INTRODUCTION

Tunnel construction in squeezing conditions is very demanding due to the difficulty in making reliable predictions of the tunnel response at the design stage. During excavation such conditions are not easily anticipated, even when driving into a specific geological formation and experience is gained on the squeezing problems encountered. Squeezing conditions may vary over short distances due to rock heterogeneity and fluctuations in the mechanical and hydraulic properties of the rock mass.

Squeezing is essentially a time dependent behaviour although for design purposes the rock mass which undergoes squeezing is often represented as an equivalent elastic-plastic medium with strength and deformability parameters which are down-graded based on observation and monitoring during excavation. The so called “short term” and “long term” conditions are often invoked, characterized by different values of the parameters involved in the constitutive model being used.

There is no doubt that under the most severe squeezing conditions an appropriate representation of the tunnel response is obtained only by using constitutive models which account for time dependent behaviour. This originates from the fact that time dependent deformations are observed whenever face advancement is stopped and these are likely to take place during

Submitted: 19 October 2009; Published: 16 November 2010

Reference: Barla, G., Bonini, M., Debernardi, D., (2010). *Time Dependent Deformations in Squeezing Tunnels*.

International Journal of Geotechnical Engineering Case Histories, <http://casehistories.geoengineer.org>, Vol.2, Issue 1, p.40-65.

doi: 10.4417/IJGCH-02-01-03.

excavation, when it is difficult to distinguish the “face effect” from the “time effect”.

This paper deals with full face excavation of large size tunnels in rock masses which exhibit squeezing behaviour. This is considered explicitly by using three constitutive models which have been validated in recent years (Barla, 2005). The case study of the Saint Martin La Porte access adit along the Lyon-Turin Base Tunnel is taken as illustration.

SQUEEZING BEHAVIOUR

The term “squeezing” originates from the pioneering days of tunnelling through the Alps. It refers to the reduction of the tunnel cross section that occurs as the tunnel is being excavated (Figure 1). Based on the work of a Commission of the International Society for Rock Mechanics (ISRM), which has described squeezing and the main features of this mechanism, it is agreed that “squeezing of rock” stands for large time dependent convergence during tunnel excavation. This happens when a particular combination of material properties and induced stresses causes yielding in some zones around the tunnel, exceeding the limiting shear stress at which creep starts. Deformation may terminate during construction or continue over a long period of time.

The magnitude of tunnel convergence, the rate of deformation, and the extent of the yielding zone around the tunnel depend on the geological and geotechnical conditions, the in situ state of stress relative to rock mass strength, the groundwater flow and pore water pressure, and the rock mass properties. Squeezing is therefore synonymous with yielding and time dependence, and often is largely dependent on the excavation and support techniques being used. If the support installation is delayed, the rock mass moves into the tunnel and a stress redistribution takes place around it. On the contrary, if deformation is restrained, squeezing will lead to long term load build-up of the support system.



Figure 1. Squeezing rock reduces the tunnel cross section in the Saint Martin La Porte access adit (Lyon-Turin Base Tunnel). The photographs show re-mining works needed in order to cope with the difficult conditions encountered.

THE SAINT MARTIN LA PORTE ACCESS ADIT

A viscoelastic-plastic model (CVISC), an elastic-viscoplastic model (VIPLA), and a more complex elastic-plastic-viscoplastic model (SHELVIP) have been used to analyze the tunnel response based on convergence monitoring in representative sections of the Saint Martin La Porte access adit. An illustration of the geological conditions and of the excavation-support system adopted in this tunnel is given below.

Geological Conditions

The first 800 m of the Saint Martin La Porte access adit (Figures 2 and 3) have been excavated in the Sub-Briançonnaise zone consisting of large folds including carbonate rocks, marl and dolomite. After crossing an alluvial deposit zone (originated by a buried paleo watercourse) the tunnel enters the Carboniferous Formation, “Zone Houillère Briançonnaise-



Unité des Encombres“, which is composed of black schists (45 to 55%), sandstones (40 to 50%), coal (5%), clay-like shales and cataclastic rocks.

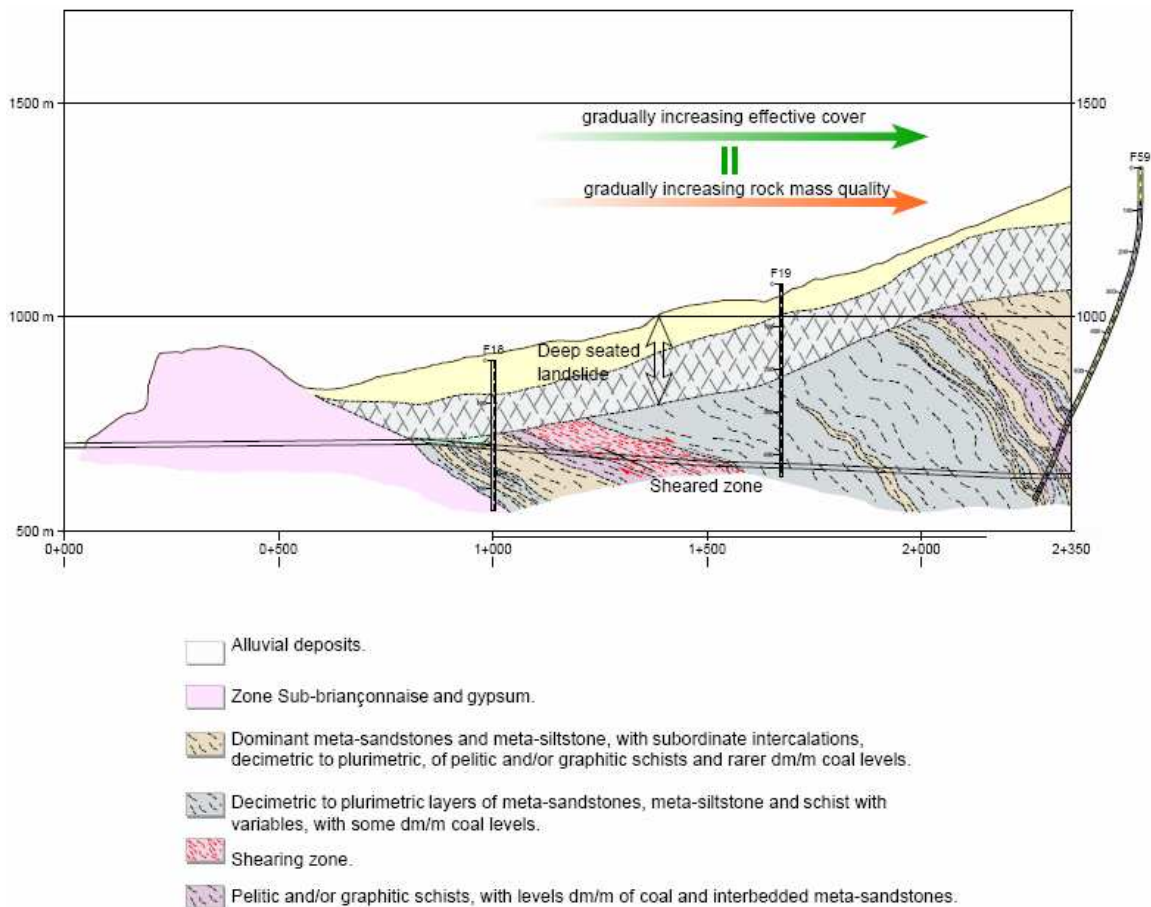


Figure 2. Geological profile along the Saint Martin La Porte access adit (modified from GDP Consultants, 2009).

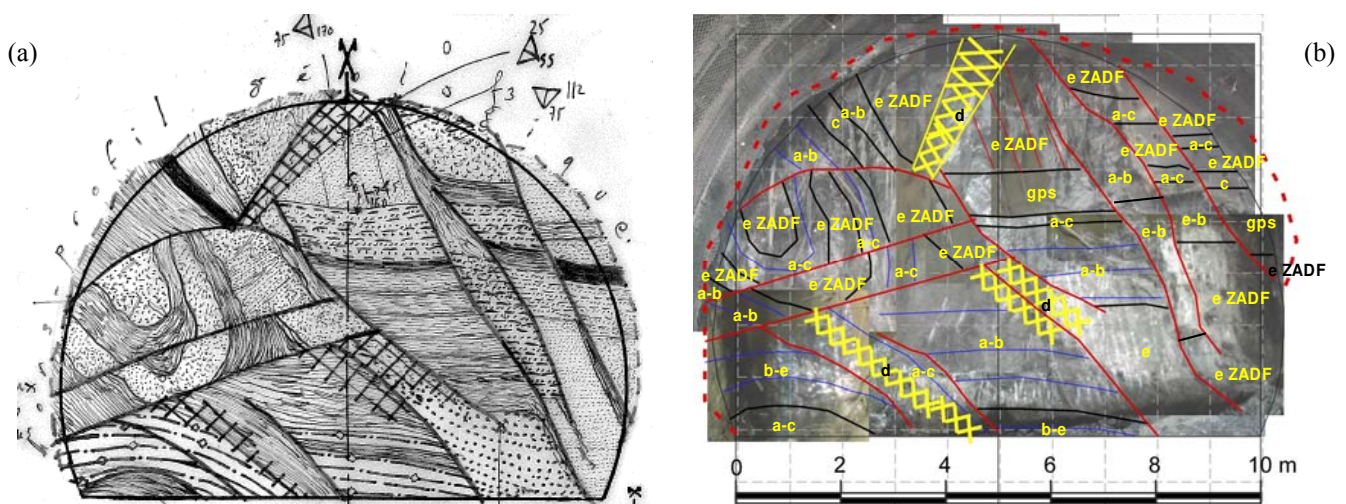


Figure 3. Typical geological conditions at the face at chainage 1545.5 m: (a) handmade sketch, (b) electronic database. a = clay shale; b = schists; c = coal; d = cataclastic rock; e = sandstone; a-b = gray clay shales; a-c = graphitic schists; b-e = schists and sandstone with pyrite; e ZADF = sandstones with alteration; gps = psammitic sandstone.



A characteristic feature of the ground observed at the face during excavation (Figure 3) is the highly heterogeneous, disrupted and fractured conditions of the rock mass which exhibits very severe squeezing problems. The rock mass is often affected by faulting that results in a degradation of the ground conditions. The overburden along the tunnel in the zone of interest ranges from 280 m to 600 m. Excavation takes place in essentially dry conditions.

A recent review of the geological data collected during the excavation of the tunnel (Martinotti, 2009) resulted in a novel interpretation of the large convergences measured between chainage 1200 and 1550 m, discussed later in paragraph 3.3. This zone is, in fact, characterised by a low thickness of the “in place” rock mass, since a significant part of the cover is part of a deep-seated landslide. Moreover, this tunnel section is characterised by extensive shearing of tectonic origin.

In order to assess the rock mass quality during excavation, detailed mapping of the geological conditions at the face was undertaken as depicted in Figure 3. This provided information on the percent distribution of “strong” (sandstones and schists) and “weak” (coal and clay-like shales) rocks at the face (Figure 4). On the basis of a detailed classification of the rock mass, the tunnel was divided into zones having homogeneous behaviour. The rock mass strength σ_{cm} , according to Hoek (2001), was used to this end as a discriminating parameter.

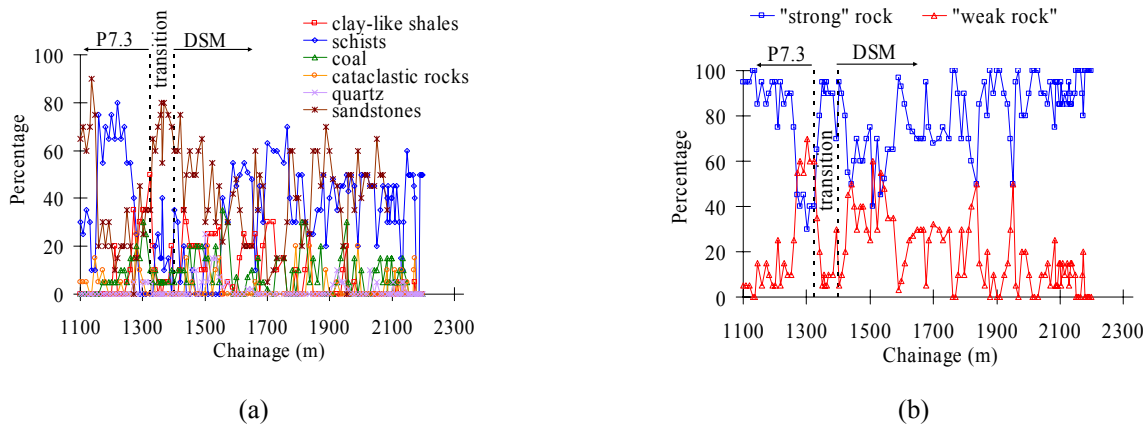


Figure 4. Percent distribution of (a) rock types and (b) “strong” (sandstones and schists) and “weak” (coal and clay-like shales) rocks at the face.

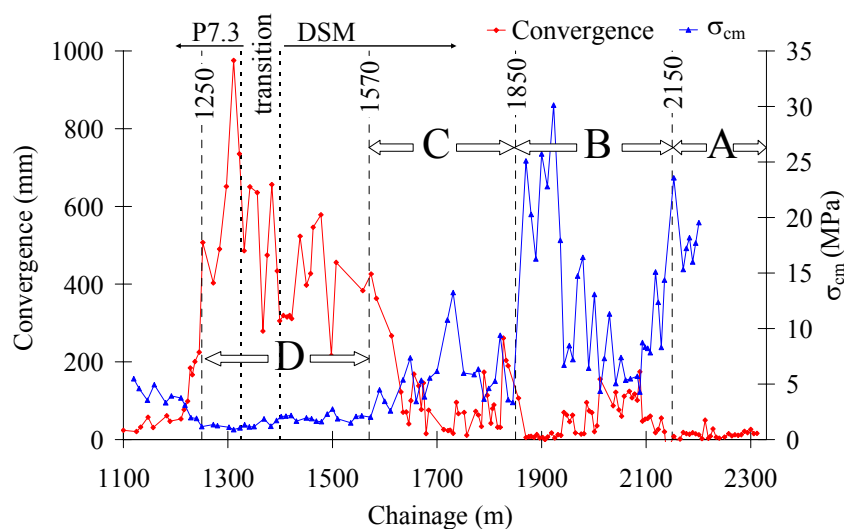


Figure 5. Correlation of convergences along array 1-5, 15 m from the face, and rock mass strength σ_{cm} , with indication of the zones with homogeneous behaviour.



Figure 5 correlates the convergence along the horizontal array (1-5), 15 m from the tunnel face, with the rock mass strength σ_{cm} indirectly determined following the relationship suggested by Hoek (2001), which relates the normalized radial displacement (u_r/r) to the normalized rock mass strength (σ_{cm}/p_0), with r = tunnel radius and p_0 = in situ stress. Following this interpretation, it is possible to identify four rock mass classes as follows:

- Class D: tectonically sheared zone;
- Class C (from 1570 to 1850 m): mixed face with pelitic and/or graphitic schists, with decimetric/metric levels of coal and subordinate intercalations of meta-sandstones;
- Class B (from 1850 to 2150 m): mixed face formed by alternations of decimetric/metric levels of meta-sandstones, meta-siltstones and shales in varying proportions, with some decimetric/metric levels of coal;
- Class A (from 2150 to 2330 m): homogeneous face consisting of meta-siltstones and sandstones, with subordinate interbedded decimetric/metric pelitic and/or graphitic schists, with rare levels of coal.

Excavation-Support Systems

Several support systems were used when excavating through the Carboniferous zone. However, it soon became apparent that a stiff support would not be feasible in the severely squeezing conditions encountered and that a yielding support system needed to be implemented. Initially, a support system consisting of yielding steel ribs with sliding joints (TH, Toussaint-Heintzmann type), rock anchors and a thin shotcrete layer in a horseshoe profile was applied in conjunction with face reinforcement by means of fibre-glass dowels (Figure 6, Section P7.3). The equivalent radius of Section P7.3 is about 5.6 m, with a total height of 10.7 m and a maximum horizontal span of 11 m. The tunnel sections with such a support system installed, up to chainage 1384 m, underwent very large deformations with convergences up to 2 m and later needed to be re-mined.

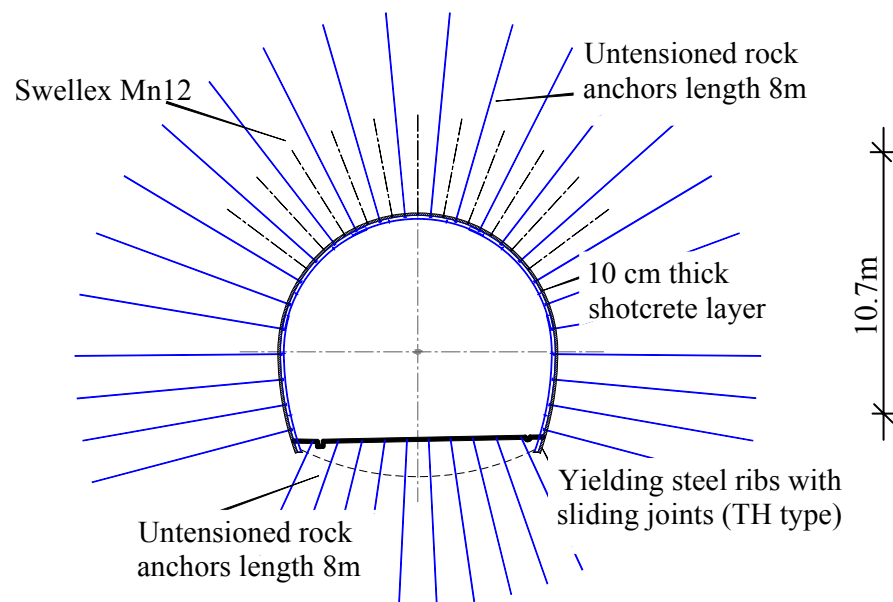


Figure 6. Tunnel cross section showing the excavation-support system P7.3 adopted between chainage 1267 and 1324 m. For sake of simplicity the face pre-reinforcement is not shown.

In order to improve the working conditions and to better control the very severe squeezing conditions encountered, an innovative yielding support system was implemented with a near circular cross section (Section DSM). The size of this cross section varied often due to the different conditions met during excavation, i.e. the maximum crown excavation radius was 6.7 m, the minimum 5.5 m. The average equivalent radius of Section DSM is about 6 m, with an average total height of 11.7 m and an average maximum horizontal span of 12.5 m. This system was initially tested along the re-mined transition



zone (from chainage 1325 m to 1384 m) and systematically adopted after chainage 1440 m. The innovative system can be summarized as follows (Figure 7):

- Stage 0: face pre-reinforcement, including a ring of grouted fibre-glass dowels around the opening, designed to reinforce the rock mass ahead and around the tunnel perimeter over a 2 to 3 m thickness.
- Stage 1: mechanical excavation carried out in steps of one meter length, with installation of a support system consisting of un-tensioned rock anchors (length 8 m) along the perimeter, yielding steel ribs with sliding joints (TH type), and a 10 cm thick shotcrete layer. The tunnel is opened in the upper cross section to allow for a maximum convergence of 600 mm.
- Stage 2: the tunnel is opened to the full circular section at a distance of 25-30 m from the face, with application of 20 cm shotcrete lining, yielding steel ribs with sliding joints (TH type) with 9 longitudinal slots (one in the invert) fitted with HiDCon (Highly Deformable Concrete) elements. The tunnel is allowed to deform in a controlled manner to develop a maximum convergence which should not exceed 400 mm.
- Stage 3: installation of a coffered concrete ring at a distance of 80 m from the face.

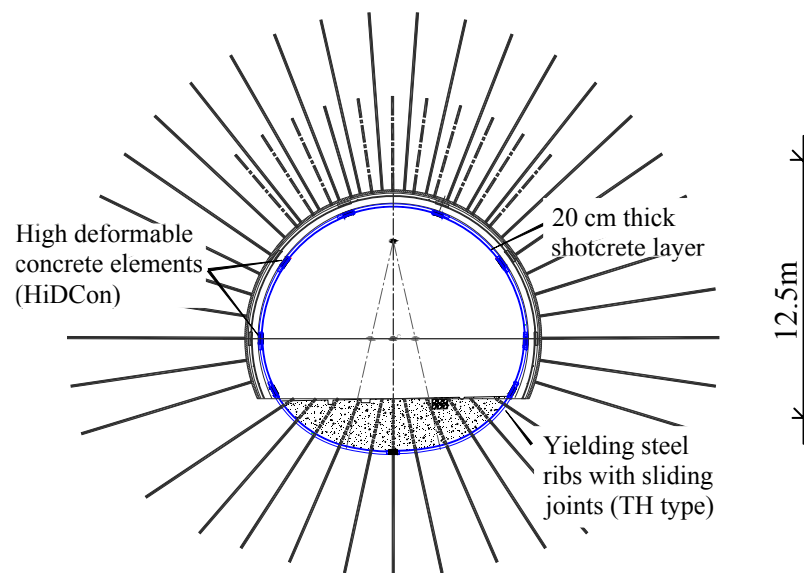


Figure 7. Tunnel cross section showing the excavation-support system DSM adopted between chainage 1400 and 1750 m with the HiDCon elements installed. Note that following chainage 1550 m the number of deformable elements installed was gradually reduced. For sake of simplicity the face pre-reinforcement is not shown.

As shown in Figures 8 and 9 the HiDCon elements are installed in slots in the shotcrete lining between the TH type steel ribs and are intended to provide the tunnel with a yielding support which allows controlled deformations to take place. These HiDCon elements are composed of a mixture of cement, steel fibres and hollow glass particles. The glass particles, which increase the void fraction of the mixture, collapse at a predetermined compressive stress, thereby providing the desired deformability of the element.

In the specific project conditions of the Saint Martin La Porte access adit the HiDCon elements adopted have a height of 40 cm, a length of 80 cm, and a thickness of 20 cm. They have been designed to yield up to 50% strain approximately in a ductile manner, while the yield strength has been chosen to be 8.5 MPa. Figure 10 shows the characteristic stress-strain diagrams obtained for such elements in laboratory tests. It is worth noting that, according to the laboratory tests, the stiffness of elements varies. This is due to the fact that only parts of the whole deformable elements could be tested by means of the available equipment. However the aim of the test was to verify the effective strain capacity of the deformable elements under constant loading. Therefore the nominal stiffness of the deformable elements was adopted into the numerical analyses (Table 1).



Figure 8. Detail of the installation of the TH steel sets and HiDCon elements.



Figure 9. Photograph of the tunnel with the DSM support system installed. The HiDCon elements inserted in the shotcrete lining are well visible.

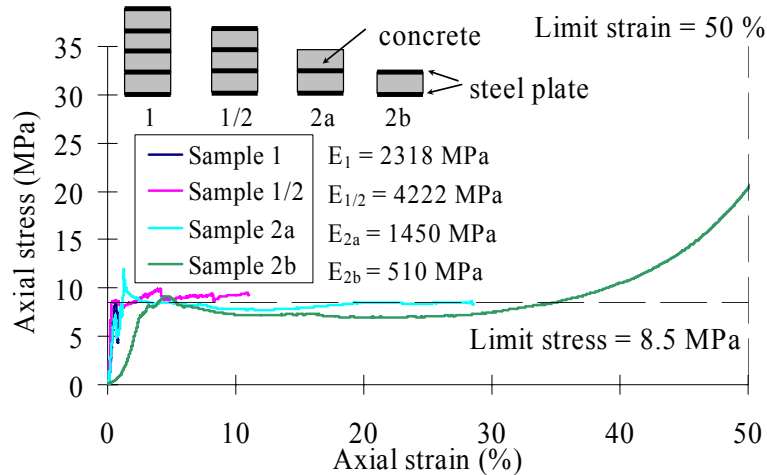


Figure 10. Characteristic stress-strain diagram of a HiDCon element.

Performance Monitoring Data

Systematic monitoring of tunnel convergence is underway along the tunnel. Convergences are measured by means of optical targets placed along the tunnel perimeter. A number of special sections have been equipped with multi-position borehole extensometers and strain meters located across the HiDCon elements. Extrusometer monitoring has been as well used to measure the longitudinal displacement ahead of the tunnel face. In addition, the strain level in the primary and final lining has been monitored (Barla et al., 2007). Table 1 provides a list of the special sections installed along the tunnel.

Table 1. Special monitoring sections installed along the Saint Martin La Porte access adit.

Chainage (m)	Extensometres		Strain level	
	HiDCon	Multi position	Primary lining	Final lining
1229				✓
1323				✓
1330		✓		
1340				
1347	✓			
1353				✓
1368				
1383				✓
1421	✓	✓	✓	
1443	✓	✓		
1457				✓
1503	✓	✓	✓	
1545				
1575		✓		
1580	✓	✓	✓	
1650	✓			
1662				✓
1704		✓		
1827				✓
1914				✓
2012		✓		✓

Figure 11 shows the convergences of section 1297 m compared with face advancement. This provides a clear example of the time-dependent behaviour of the rock mass with convergence rates depending on the advancement rate and face stops. In the following, the example of monitoring performance of section at chainage 1443 m is taken as representative of the tunnel behaviour in the tectonically sheared zone.

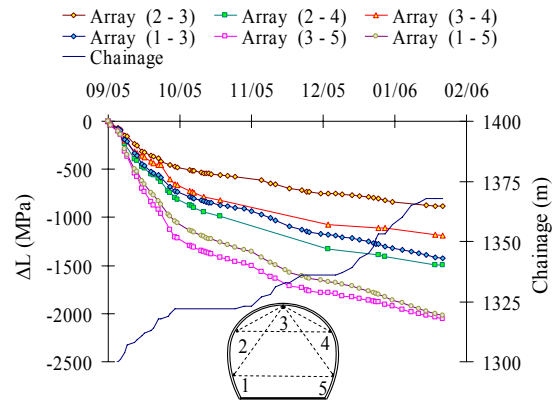


Figure 11. Convergences of section 1297m versus face advancement.

Since the optical targets are installed at a minimum distance of 1 m from the tunnel face and the multi-position borehole extensometers at a greater distance from it, the tunnel displacements occurring ahead of the face, within the so called “core”, and at the same face are lost. An accurate estimate of the displacement loss is not possible but a reasonable value for such an estimate is thought to be about 50% of the total displacement.

In order to gain in the understanding of the tunnel response, it is of interest to consider Figure 12, which shows the tunnel displacement that has occurred in stage 1 along arrays 1-3, 3-5 and 1-5 between chainage 1100 m and 2250 m, with the tunnel face being 15 m ahead of the monitoring section. The black solid line shows the 600 mm displacement limit. Also illustrated in Figure 13 are the convergences measured along array 1-5 in stage 2 after 30, 80 and 120 days from the stage 2 installation. Many stops of face advance, represented in the figures by vertical lines, took place along the tunnel length with the DSM cross section implemented, due to technical and contractual reasons.

The following observations can be made:

- The large deformations in conjunction with typical anisotropic responses of the rock mass are associated with cross section P7.3 between chainages 1200 and 1384 m; with cross section DSM the convergences in stage 1 are smaller with the tunnel strain never in excess of 600-700 mm (6-7%).
- The 600 mm allowed convergence in stage 1 is exceeded locally, due to the stop of face advance and to the very poor quality of the rock mass encountered; in such cases re-shaping of the tunnel cross section took place before installing the composite lining adopted in stage 2.
- The tunnel deformation associated with cross section P7.3 appears to be rather different in one section with respect to the neighbouring one, which is not the case for cross section DSM.
- At chainage 1550 m approximately, the tunnel response appears to exhibit smaller convergences in line with the generally improved rock mass conditions encountered.

The data provided by the multi-position borehole extensometers, installed in eight sections of the tunnel (Table 1), were useful to determine the strain distribution around the excavation. The performance exhibited at chainage 1443 m (Figures 14 and 15) is of main interest for the understanding of the tunnel behaviour. Figure 14 shows the radial displacement versus the distance from the tunnel perimeter along six directions, as measured on October 24th, 2006 (last measurement in stage 1, 33 days after excavation) and March 6th, 2007 (last measurement in stage 2 before installing the final lining, 166 days after excavation). Figure 15 underlines the zone with strain greater than 1% around the tunnel and at the end of stage 1 and before the installation of the final lining.

It is of interest to observe the asymmetric response of the tunnel (displacements are higher at the crown and right side, typically extending 1 tunnel diameter), caused by the generally nonsymmetric and anisotropic structure of the rock mass with respect to the tunnel axis (Figure 15) and the significant displacements occurring in stage 2 due to the presence of the deformable elements.

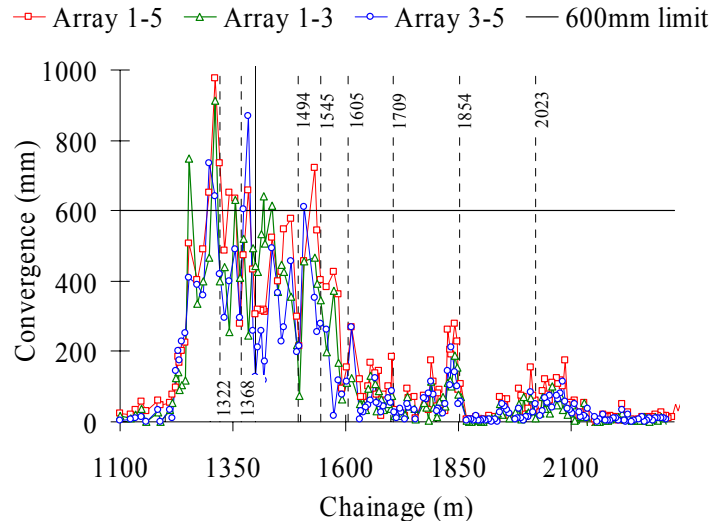


Figure 12. Convergences along arrays 1-3, 3-5 and 1-5, 15 m from the face, in stage 1.

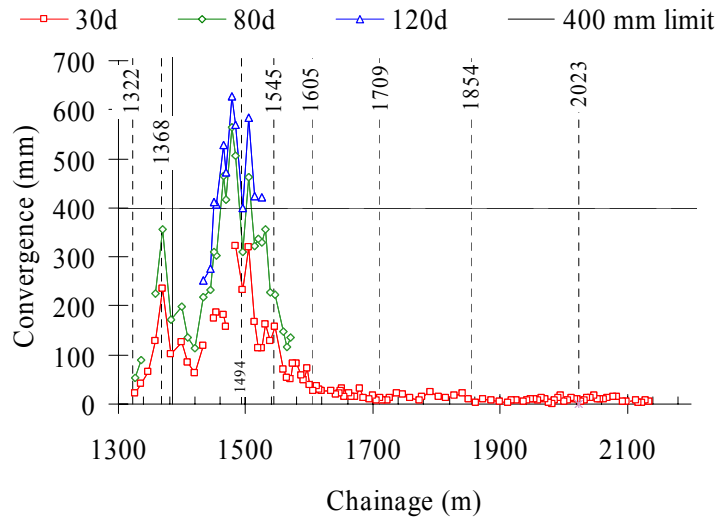


Figure 13. Convergences 30, 80 and 120 days following excavation with stage 2 installed.

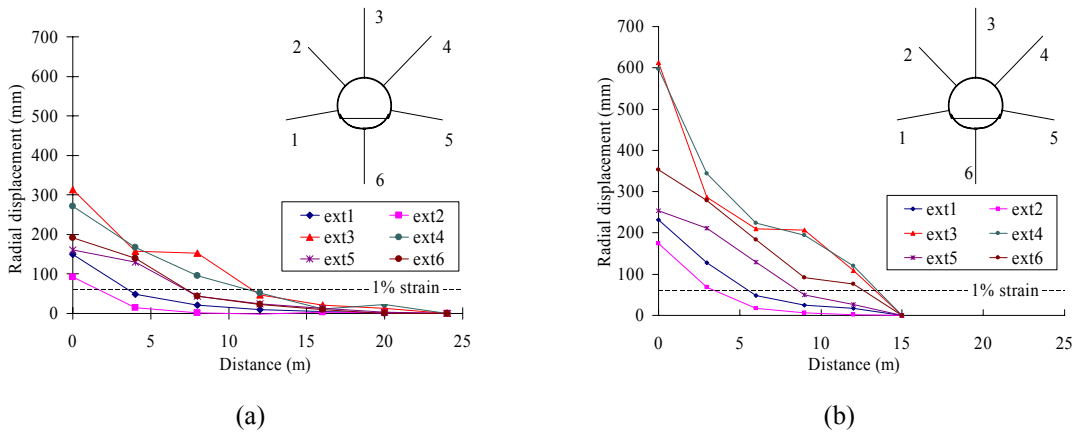


Figure 14(a). Radial displacement from multi-position borehole extensometers at chainage 1443 m on October 24th, 2006 (left) and March 6th, 2007 (right).

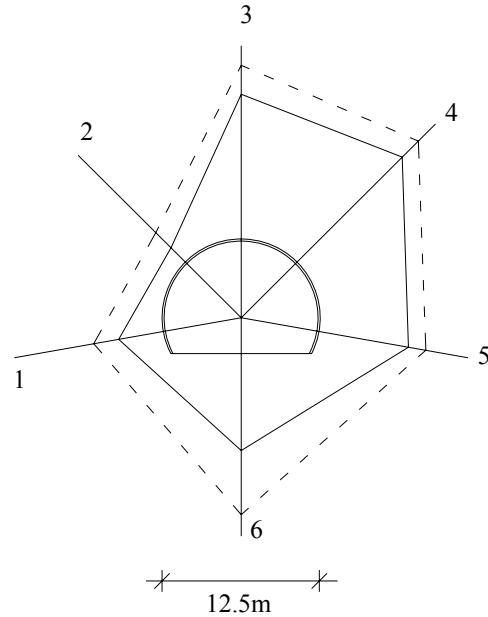


Figure 15. Multi-position borehole extensometers at chainage 1443 m: 1% strain at the end of stage 1 (dashed line) and before the installation of final lining (solid line).

Figure 16 shows the shortening of the deformable elements installed at chainage 1443 m as measured by strain meters installed across them. The measurements started on November 1st, 2006, about 5 days after the completion of stage 2 and ended on February 27th, 2007. As already noted for the multi-position borehole extensometers, the behaviour of the cross section is again asymmetric, with greater convergences on the right side of the tunnel. It is observed that about 50 days after installation elements 6 and 7 underwent rotation and buckling, despite the level of strain attained (about 40 and 19% respectively assuming a length of the extensometer equal to 250 mm) being lower than the limit value (50%). Figure 17 gives a photograph of element 6 before installation of the final lining.

Figure 18 shows the tangential stress in the final lining at chainage 1457 m, which is the section closest to chainage 1443m. These stresses are observed to gradually increase over a period of 2.5 years, reaching a maximum value equal to 10.8 MPa (maximum values are at the sidewalls), with an average value of 7.0 MPa. As illustrated in Figure 19, the stresses in the final lining are generally influenced by the excavation/construction sequence. For example, the stiff supported sections at chainages 1229 and 1323 m exhibit greater stress values than other sections where the yielding support system was adopted.

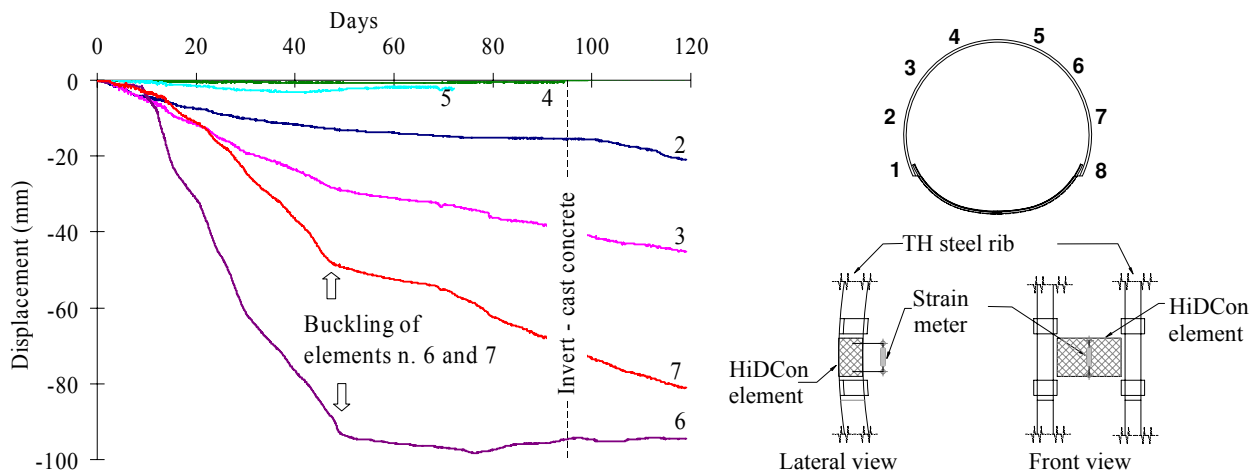


Figure 16. Shortening of the HiDCon elements at chainage 1443 m (from strain meters).



Figure 17. Detail of deformable element 6 at chainage 1443 m prior to casting of final lining.

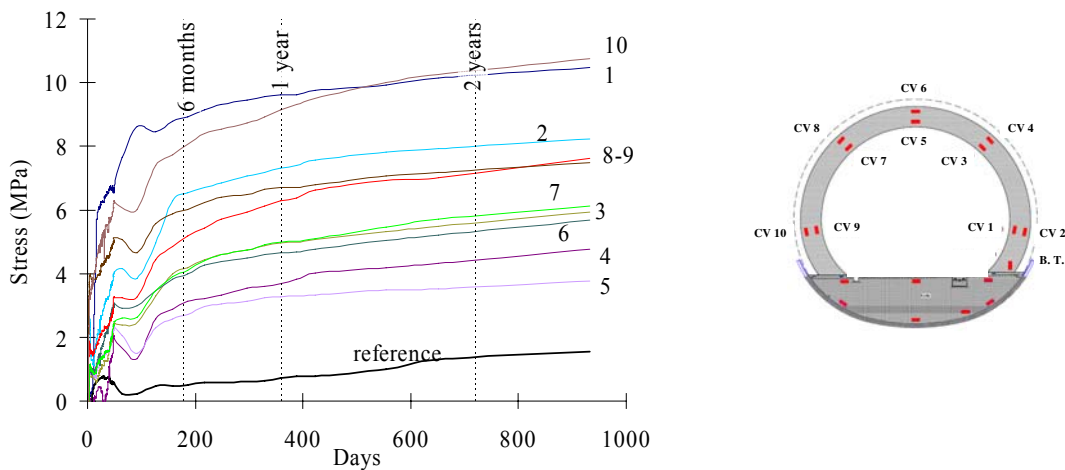


Figure 18. Stresses in final lining at chainage 1457 m.

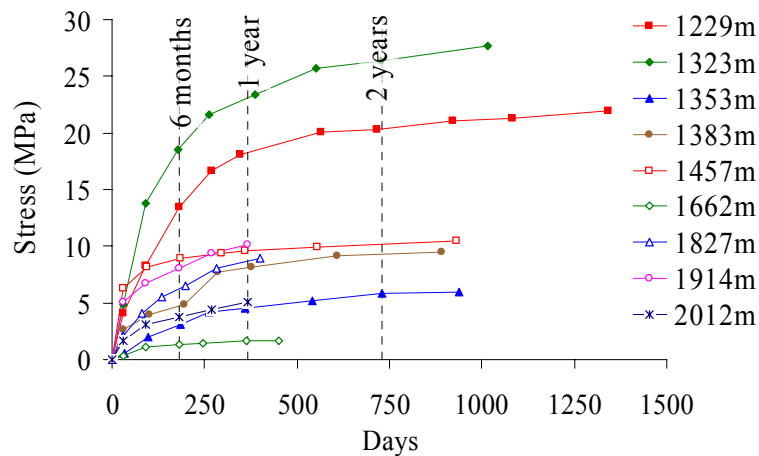


Figure 19. Maximum tangential stress in final lining at different chainages.



TIME-DEPENDENT CONSTITUTIVE MODELS

In order to describe the tunnel response associated with severely squeezing conditions, time dependent constitutive models need be used. In the following a viscoelastic-plastic model (CVISC), an elastic-viscoplastic model (VIPLA) and a more complex elastic-plastic-viscoplastic model (SHELVIP) are briefly described.

CVISC Model

The CVISC model (Itasca, 2006) is an analogical model which couples, in series, the Burgers viscoelastic model (i.e. Kelvin and Maxwell models in series) with a plastic flow rule, based on the Mohr-Coulomb yield criterion, as shown in Figure 20.

The volumetric behaviour is only elastic-plastic and is governed by the linear elastic law and the plastic flow rule (Figure 20a), while the deviatoric behaviour is viscoelastic-plastic and is driven by the Burgers model and the same plastic flow rule (Figure 20b). This means that the viscoelastic strains are deviatoric and depend only on the deviatoric stress state; instead the plastic strains are both deviatoric and volumetric and depend on the global stress in accordance with the chosen flow rule.

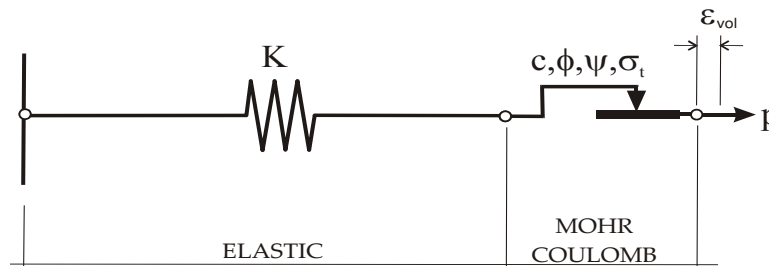


Figure 20(a). CVISC model: volumetric behaviour.

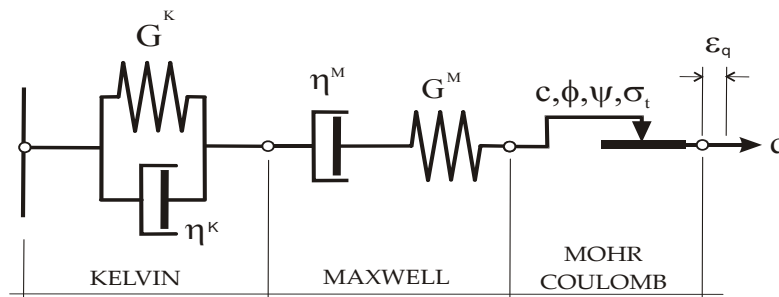


Figure 20 (b). CVISC model: deviatoric behaviour.

VIPLA Model

The VIPLA model (Lemaitre and Chaboche, 1996) is based on Perzyna's overstress theory (Perzyna, 1966) which states that the strain rate tensor $\dot{\epsilon}_{ij}$ can be split into elastic $\dot{\epsilon}_{ij}^e$ and viscoplastic $\dot{\epsilon}_{ij}^{vp}$ components, to give:

$$\dot{\epsilon}_{ij} = \dot{\epsilon}_{ij}^e + \dot{\epsilon}_{ij}^{vp} \quad (1)$$

The viscoplastic strain rate tensor $\dot{\epsilon}_{ij}^{vp}$ can be calculated by the following flow rule:

$$\dot{\epsilon}_{ij}^{vp} = \gamma \cdot \Phi(\langle F \rangle) \cdot \frac{\partial g}{\partial \sigma_{ij}} \quad (2)$$

where γ is the fluidity parameter, F is the over-stress function, representing the distance from the yield surface $f = 0$, $\Phi(\langle F \rangle)$ is the so-called viscous nucleus, g is the viscoplastic potential and σ_{ij} the stress tensor.



The time dependency is introduced in this model by modifying the classical flow rule of elastoplasticity and by discarding the consistency rule ($df = 0, f \leq 0$), thus allowing the yield function f to be positive or negative. The viscoplastic potential g defines the direction of $\dot{\varepsilon}_{ij}^{vp}$, while F influences its modulus by means of the viscous nucleus Φ .

In the VIPLA model F is assumed to be represented by the yield function f and Φ is assumed to be a power law:

$$\Phi = \langle F \rangle^n = \langle f \rangle^n \quad (3)$$

where n is a constitutive parameter ($n \geq 1$).

The yield function f is split into a part \bar{f} which depends only on the stress state, and a part K , which depends only on the viscoplastic strain, according to:

$$f = \frac{\bar{f}(\sigma_{ij})}{\kappa(\varepsilon_{ij}^{vp})} \quad (4)$$

For the function the Von Mises yield criterion is assumed:

$$\bar{f}(\sigma_{ij}) = q \quad (5)$$

where q is the stress deviator.

A potential hardening is introduced by means of the function K :

$$\kappa(\varepsilon_{ij}^{vp}) = (\varepsilon_q^{vp})^{-m/n} \quad (6)$$

where m is a constitutive parameter ($1 - n < m \leq 0$) and ε_q^{vp} is the deviatoric viscoplastic strain, $\varepsilon_q^{vp} = \sqrt{4/3 \cdot J_{2,\varepsilon^{vp}}}$ where $J_{2,\varepsilon^{vp}}$ is the second invariant of the viscoplastic strain deviator.

Under these assumptions, the yield surface $f = 0$ is reduced to the hydrostatic axis and it does not change with time.

The viscoplastic potential g is taken to be equal to \bar{f} (i.e. the flow rule is associated). With these assumptions, the viscoplastic strains depend only on the deviatoric stress state and do not induce volumetric strains. Therefore, Eqn. (2) becomes:

$$\dot{\varepsilon}_{ij}^{vp} = \frac{3}{2} \cdot \gamma \cdot q^{n-1} \cdot (\varepsilon_q^{vp})^m \cdot s_{ij} \quad (7)$$

The constitutive parameters n and m define respectively the dependence of the viscoplastic strain rate tensor on the deviatoric stress and on the equivalent viscoplastic strain, whereas the parameter γ defines the amplitude of the viscoplastic strains.

SHELVIP Model

The SHELVIP model (Stress Hardening ELastic Viscous Plastic model) is derived from the Perzyna's overstress theory, by adding a time independent plastic component (Debernardi and Barla, 2009; Debernardi, 2008). Therefore it is possible to split the strain rate tensor $\dot{\varepsilon}_{ij}$ into elastic $\dot{\varepsilon}_{ij}^e$, plastic $\dot{\varepsilon}_{ij}^p$, and viscoplastic $\dot{\varepsilon}_{ij}^{vp}$ components, to give:

$$\dot{\varepsilon}_{ij} = \dot{\varepsilon}_{ij}^e + \dot{\varepsilon}_{ij}^p + \dot{\varepsilon}_{ij}^{vp} \quad (8)$$

According to the classical theory of elastoplasticity, the time independent plastic strains ε_{ij}^p develop only when the stress point reaches the plastic yield $f_p = 0$ surface (Figure 21), defined by the Drucker-Prager criterion:

$$f_p = q - \alpha_p \cdot p - k_p \quad (9)$$



The plastic strain rates $\dot{\varepsilon}_{ij}^p$ can be evaluated using the classical flow rule of elastoplasticity:

$$\dot{\varepsilon}_{ij}^p = \lambda \cdot \frac{\partial g_p}{\partial \sigma_{ij}} \quad (10)$$

where g_p is the plastic potential, $g_p = q - \omega_p \cdot p$, that defines the direction of $\dot{\varepsilon}_{ij}^p$, ω_p is the plastic dilatancy and λ is the plastic multiplier, that can be determined using the consistency condition $df_p = 0, f_p \leq 0$.

The viscoplastic strain rates $\dot{\varepsilon}_{ij}^{vp}$ develop only if the effective stress state exceeds a viscoplastic yield surface $f_{vp}=0$ (Figure 21) which is also defined by the Drucker-Prager criterion. This surface is internal to the plastic yield surface and intersects the p -axis at the same point as the plastic yield surface. Thus, it is possible to write:

$$f_{vp} = q - \alpha_{vp} \cdot \left(p + \frac{k_p}{\alpha_p} \right) \quad (11)$$

where α_{vp} is a visco-hardening parameter that defines the internal viscous state of the material.

The viscoplastic strain rate $\dot{\varepsilon}_{ij}^{vp}$ can be determined using the flow rule of Perzyna's overstress theory:

$$\dot{\varepsilon}_{ij}^{vp} = \gamma \cdot \Phi (\langle F \rangle) \cdot \frac{\partial g_{vp}}{\partial \sigma_{ij}} \quad (12)$$

The overstress function F is assumed to be equal to the viscoplastic yield function f_{vp} and the viscous nucleus Φ to be a power law:

$$\Phi = \langle F \rangle^n = \langle f_{vp} \rangle^n \quad (13)$$

where n is a constitutive parameter.

The viscoplastic potential g_{vp} is assumed to be $g_{vp} = q - \omega_{vp} \cdot p$, where ω_{vp} is the viscoplastic dilatancy. The hardening of the viscoplastic yield surface is governed by the differential equation:

$$\dot{\alpha}_{vp} = \frac{l}{m \cdot n} \cdot \frac{f_{vp}}{p + k_p/\alpha_p} \cdot \left(\frac{f_{vp}}{q} \right)^{n \cdot m} \quad (14)$$

where m and l are constitutive parameters.

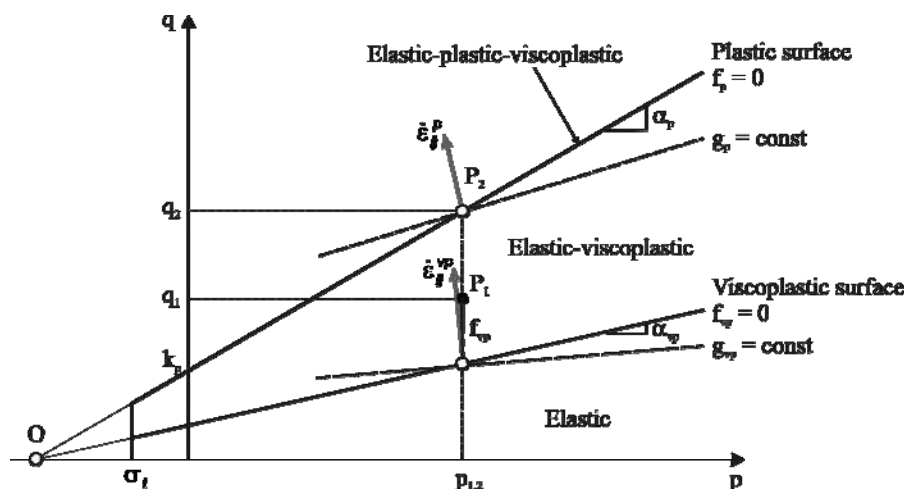


Figure 21. SHELVIP model in the p - q stress plane.



MODELLING OF THE TUNNEL RESPONSE

The three constitutive models described above were adopted in order to back-analyze the tunnel response in terms of convergence monitored during excavation. The final purpose of this study is to see how three different time-dependent constitutive models, with different levels of complexity, can reproduce the time dependent deformations of the tunnel. The information provided is of relevance in relation to numerical modelling of the tunnel response in severe to extreme squeezing conditions, with acceptable level of confidence, and to the need to optimize the type of support adopted and the excavation/support sequence implemented.

It is noted that the numerical analyses presented in this paper follow the chronological sequence of the research work carried out by the authors. As a consequence the level of complexity of the analyses performed is gradually increased. The modelling in plane strain conditions with the CVISC model is described first. Then, the semi-analytical solution based on the VIPLA model and the numerical solution in axisymmetric conditions with the SHELVIP model are illustrated.

The starting values of the constitutive parameters used in the back-analyses were determined based on the results of laboratory tests. Coal samples directly obtained from blocks at the tunnel face or borehole cores were subjected to uniaxial, triaxial, creep and relaxation tests (Debernardi, 2008). Since laboratory testing is characterised by a short time duration, with respect to both the construction and operation time, the viscous properties obtained in the laboratory were intended as short term parameters.

The mechanical properties at laboratory scale were then scaled to obtain the rock mass parameters. The elastic and plastic parameters were scaled accordingly to standard rock mechanics procedures. The viscous parameters were increased in stages to account for geometry, scale of the problem, stress level and distribution of rocks at the face with time-dependent behaviour. Due to the long computation time needed, only with the semi-analytical solution and the VIPLA model a numerical optimization procedure could be used, otherwise the constitutive parameters were modified in steps so as to fit the tunnel convergence data.

Numerical Analyses with the CVISC Model

For the purpose of numerical modelling with the CVISC model the DSM cross section at chainage 1443 m, with an equivalent radius equal to 6 m, was chosen. The numerical model was set up by using the Finite Difference Method (FDM) and the FLAC code (Itasca, 2006).

Figure 22 shows the two dimensional FDM grid with a total size of 120×120 m. It comprises a total of 20,304 4-noded quadrilateral zones and is very finely discretised near the excavation perimeter and in the lining, where the typical size is $0.1 \text{ m} \times 0.05 \text{ m}$, so that 4 elements are included in the lining thickness. The analyses were performed by accounting for large strains.

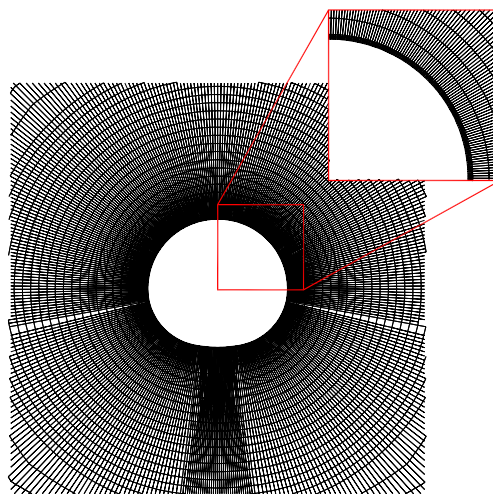


Figure 22. Detail of the FDM grid used for plane strain modelling of the tunnel response with CVISC.



The model allowed for simulation of the excavation/construction sequence. Overall five simulation steps were implemented in order to represent this as accurately as possible. Following initialization, the excavation of the top heading was simulated with a stress relaxation equal to 87% of the initial stress state. The presence of the rock dowels around the tunnel and of the primary lining was simulated with 100 kPa uniform pressure applied at the tunnel boundary. The ground was initially taken as elastic perfectly plastic and the time dependent behaviour was simulated by running the CVISC model (Table 2) for 23 days after the excavation with the intent to match the tunnel response as observed through monitoring.

Table 2. Constitutive parameters (CVISC model and lining in stage 2).

Ground (CVISC model)			Lining in stage 2			
Bulk modulus, K	942	MPa	Shotcrete	HiDCon		
Cohesion, c	0.61	MPa	Young modulus, E	20000	4000	MPa
Friction angle, ϕ	28	°	Poisson's ratio, ν	0.20	0.20	-
Dilatancy angle, ψ	0	°	UCS, σ_c	32.00	8.50	MPa
Tensile strength, σ_t	8.50E-03	MPa	Tensile strength, σ_t	3.20	0.85	MPa
Maxwell shear modulus, G^M	566	MPa	Cohesion, c	9.20	2.45	MPa
Maxwell viscosity, η^M	27.98	MPa-year	Friction angle, ϕ	30	30	°
Kelvin viscosity, η^K	4.26	MPa-year				
Kelvin shear modulus, G^K	498.1	MPa				

Following invert excavation, with the rock mass behaviour assumed as elastic perfectly plastic, the stage 2 lining was activated and the stress relaxation process completed. The lining was modelled by using quadrilateral elements with elastic behaviour. The presence of the HiDCon elements incorporated in it was simulated with quadrilateral elements with a linearly elastic ideally plastic behaviour (Table 2).

An interface was introduced between the lining and the rock surround with normal (k_n) and shear (k_s) stiffness equal to $3.45E+03$ MPa/m and $3.45E+02$ MPa/m respectively. The analysis was run with the CVISC model activated for 67 days with the intent to reproduce the observed tunnel response versus time with the convergence curve taken as target.

Figure 23 shows the computed convergence plot versus time obtained for the cross section of interest and for a total duration of 80 days. It is shown that when the model simulates the tunnel “short term” response, at the end of stage 1 (23 days after excavation) the convergence along array 1-5, namely 314 mm, is close to the in situ value (336 mm).

As expected, the model does not predict the observed deformation thereafter, when the tunnel is shown to exhibit a gradual decrease in the rate of convergence, reaching a near stable condition. This is essentially due to the rather simple mathematical formulation of the CVISC model, where the ‘long term’ time dependent behaviour of the rock mass is described by using a linear dashpot only.

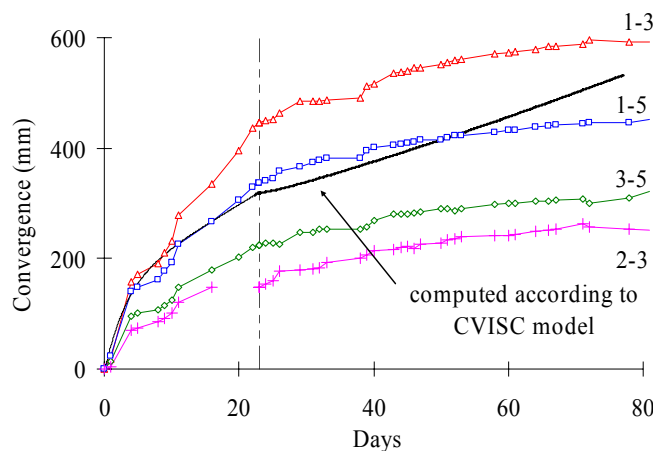


Figure 23. Computed (CVISC model) versus monitored convergence at chainage 1406 m (DSM).



Numerical Analyses with the VIPLA Model

With the intent to overcome the limitations of the CVISC model in reproducing the observed time dependent response of the tunnel, the VIPLA model was subsequently adopted. To evaluate the aptitude of this model to cope with the time dependent problem, the semi-analytical solution proposed by Nguyen-Minh and Pouya (1992) was used and implemented into the MATLAB code, however with the addition of the face influence as described below.

The main assumptions of the semi-analytical solution are as follows: (a) the tunnel is of circular section, is not lined and is at depth; (b) plane strain conditions are applied; (c) the initial stress state is isotropic and homogeneous; the ground is homogeneous, isotropic, and incompressible ($\nu=0.5$). Under these assumptions the radial viscoplastic strain rate $\dot{\epsilon}_r^{vp}$ at the distance r from the tunnel centre at time t is given by the following expression:

$$\frac{\partial}{\partial \tau} \left(\frac{\epsilon_r^{vp}}{\epsilon_R^e} \right)^{\frac{1}{\alpha}} = \left\{ u \left[1 + (\beta - 1) u^{\beta-1} \tau^\alpha \right]^{\frac{1}{1-\beta}} + u^{\frac{1}{\beta}} \frac{1}{\beta} \left\{ 1 - \left[1 + (\beta - 1) u^{\frac{\beta-1}{\beta}} \tau^\alpha \right]^{\frac{1}{1-\beta}} \right\} \right\}^{\frac{\beta}{\alpha}} \quad (15)$$

where:

$$\alpha = \frac{1}{1-m}; \beta = \frac{n}{1-m}; a = \left(\frac{\gamma}{\alpha} \right)^\alpha; \tau = t / \left(\frac{\epsilon_R^e}{a_{cyl} (2\sigma_0)^\beta} \right)^{\frac{1}{\alpha}}; \epsilon_R^e = \frac{3\sigma_0}{2E}; a_{cyl} = a \left(\frac{\sqrt{3}}{2} \right)^{\beta+1}; u = \left(\frac{R}{r} \right)^2 \quad (16)$$

with R being the tunnel radius, σ_0 the isotropic stress state, ϵ_R^e the elastic radial strain at tunnel contour, E the elastic modulus, γ , m and n the constitutive parameters of the VIPLA model. With a double numerical integration, over time and over the radial distance, it is possible to obtain the tunnel radial displacement.

In order to account for the influence of the face on the tunnel radial displacement, the isotropic stress state need be reduced according to (Panet, 1995):

$$\frac{\bar{\sigma}_0}{\sigma_0} = 0.28 + 0.72 \cdot \left(1 - \frac{0.84}{0.84 + x/R} \right) \quad (17)$$

where x is the distance from the face and $\bar{\sigma}_0$ the reduced isotropic stress state which accounts for the face influence.

The semi-analytical solution was used to fit, by means of the optimization procedure proposed by Lagarias et al. (1998), the radial displacement of the tunnel monitored both at section 1311 m, in which the P7.3 support system was installed, and at section 1444 m, where the DSM support system was used.

Support System P7.3

The equivalent radius for the tunnel cross section is 5.5 m. With the overburden depth of 310 m at chainage 1311 m, the isotropic stress σ_0 is 8.4 MPa. The rock mass elastic modulus is assumed to be 1180 MPa. With the influence of the primary lining and of the reinforcement system being neglected, the excavation sequence was simulated in detail including the “stand still” events.

By using the above semi-analytical solution and the fitting procedure implemented, the mean radial displacements observed in the section of interest were described in detail as shown in Figure 24. The computed values are shown to reproduce satisfactorily the observed behaviour over a time span of 160 days, notwithstanding the scattering of the monitoring data. The viscoplastic constitutive parameters used are summarised in Table 3.

It is of interest to note that the semi-analytical solution was also used with the constitutive parameters shown in Table 3 in order to describe the radial displacement distribution around the tunnel monitored with the multipoint borehole extensometers installed at chainage 1330 m. As illustrated in Figure 25, the observed behaviour is well described by the computed values.



Table 3. Constitutive parameters (VIPLA model) ((*) time in year and pressure in kPa).

Section 1311 m (P7.3)			Section 1443 m (DSM)		
Young's modulus, E	1180	MPa	Young's modulus, E	1180	MPa
Poisson's ratio, ν	0.5	-	Poisson's ratio, ν	0.5	-
Fluidity parameter, γ	6.63E-21	(*)	Fluidity parameter, γ	1.06E-29	(*)
Shape factor, m	-1.33	(*)	Shape factor, m	-0.92	(*)
Load dependency, n	4.88	(*)	Load dependency, n	7.28	(*)

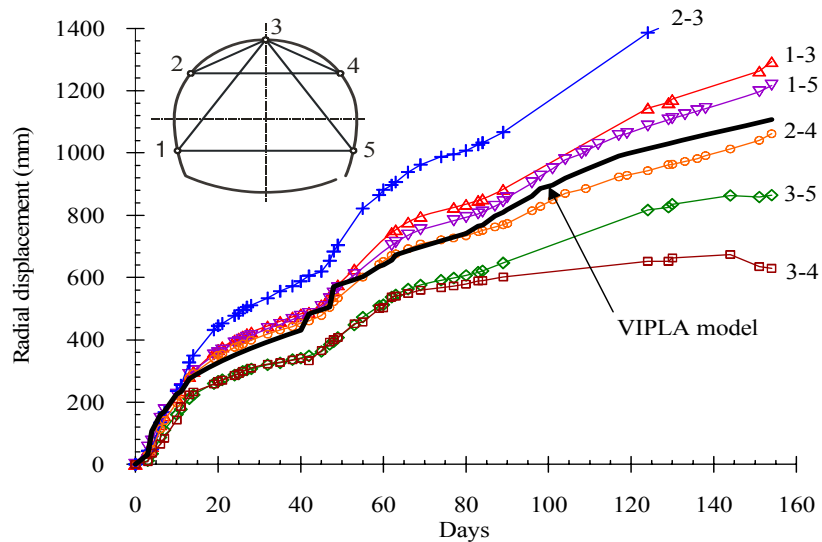


Figure 24. Computed (VIPLA model) versus monitored radial displacements at chainage 1311 m (P7.3).

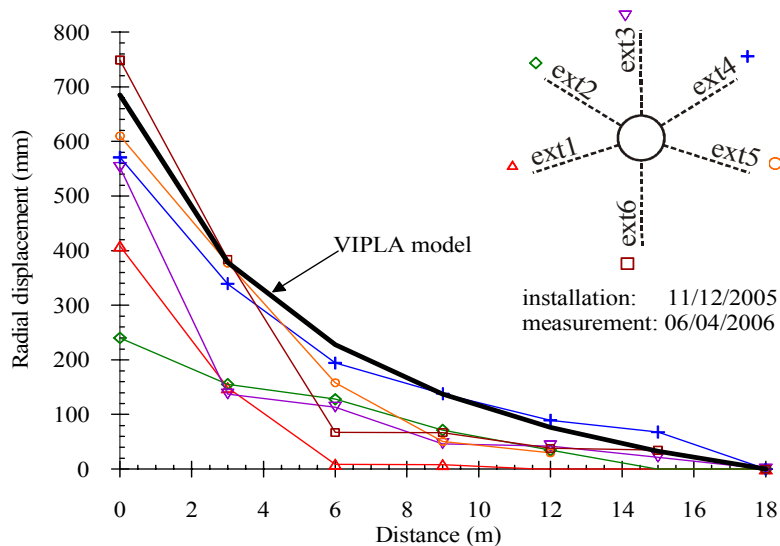


Figure 25. Computed (VIPLA model) versus monitored radial displacements from multi-position borehole extensometers at chainage 1330 m (P7.3).

Support System DSM

The DSM cross section at chainage 1443 m is given an equivalent radius of 6.0 m, with an overburden depth of 363 m and an isotropic stress σ_0 equal to 9.8 MPa. The rock mass elastic modulus is 1180 MPa. The simulation was carried out by

neglecting the primary lining and reinforcement system, due to the assumptions inherent with the semi-analytical solution, and by reproducing the excavation sequence in detail.

The results obtained by using the above semi-analytical solution and the fitting procedure are shown to describe the radial displacements at the tunnel contour very satisfactorily as illustrated in Figure 26. The viscoplastic constitutive parameters used are given in Table 3. It is shown that these same parameters and the semi-analytical solution also reproduce very accurately the extensometers measurements monitored at chainage 1444 m.

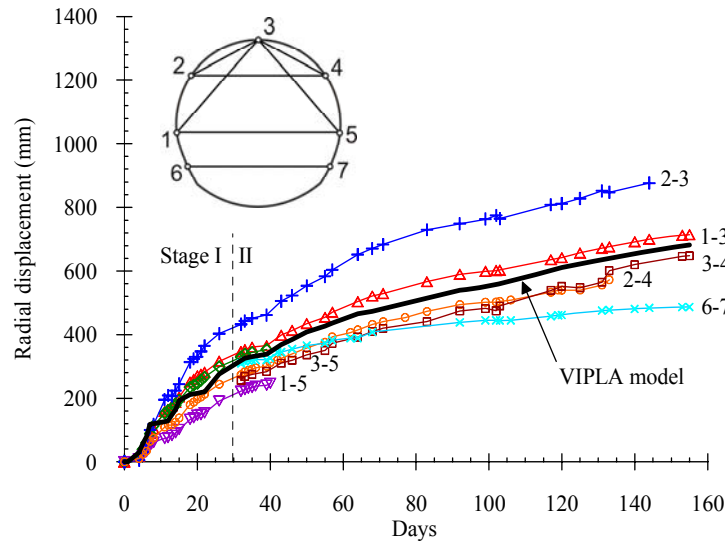


Figure 26. Computed (VIPLA model) versus monitored radial displacements at chainage 1443 m (DSM).

The results obtained for both the P7.3 and DSM sections highlight that the VIPLA model (Figure 27) reproduces the time dependent tunnel response more satisfactorily than the CVISC model, also considering that a semi-analytical solution for a circular tunnel was used. The main limitation of the VIPLA model is found in the absence of a true plastic limit that cannot be exceeded by the effective state of stress in the rock mass. This is not a very significant drawback as long as one is to describe the time dependent deformations around the tunnel. This is however not the case if one is to compute the state of stress in the lining.

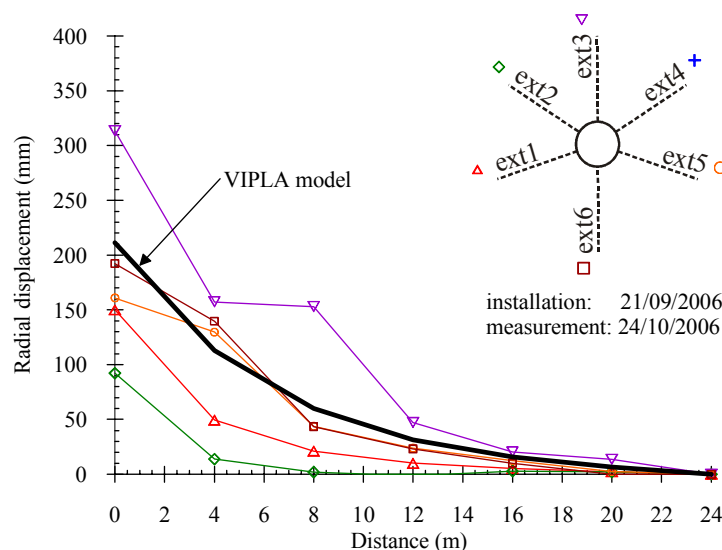


Figure 27(A). Stage I: Computed (VIPLA model) versus monitored radial displacements from multi-position borehole extensometers at chainage 1443 m (DSM).

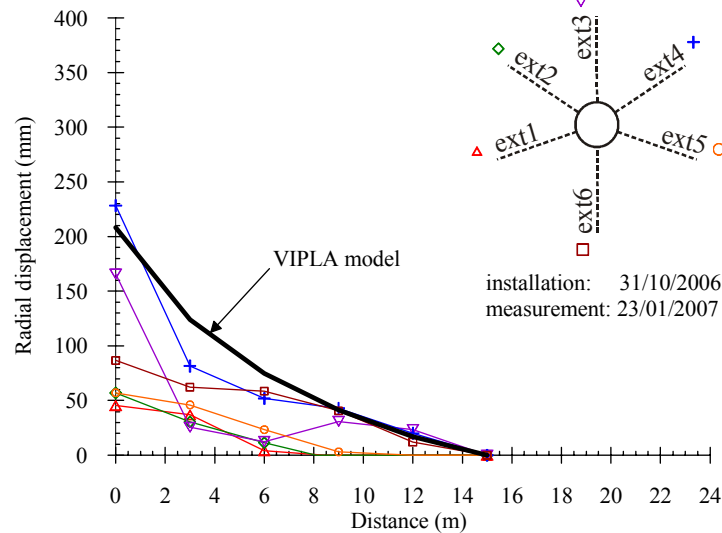


Figure 27(B). Stage II: Computed (VIPLA model) versus monitored radial displacements from multi-position borehole extensometers at chainage 1443 m (DSM).

Numerical Analyses with the SHELVIP Model

With the intent to overcome the limitations of the CVISC and VIPLA constitutive models in modelling the tunnel response as outlined above, the newly developed SHELVIP model (Debernardi and Barla, 2009; Debernardi, 2008) was adopted. This model was first validated against the results of creep and stress relaxation tests carried out on coal samples obtained from boreholes drilled near the tunnel axis (Debernardi, 2008; Barla et al., 2009).

Particular attention was again given to the modelling of sections with both support systems P7.3 and DSM. The numerical analyses of the tunnel response were performed by using the Finite Difference Method (FDM) and the FLAC code (Itasca, 2006) with the SHELVIP model implemented. In both cases axisymmetric conditions were assumed in order to better reproduce the three-dimensional influence of the tunnel face, which is known to play a significant role in squeezing conditions. The large deformations option as available in FLAC was used.

The tunnel cross section is taken as circular. Figure 28 shows the FDM grid adopted. The mesh is composed of square elements, with size increasing gradually from 0.5 to 4 m when moving from the near vicinity of the tunnel outwards. The total size of the grid (184 - 92 m) is now very extended in order to minimize the boundary effects that are very significant in the case of large deformations. Again particular attention was posed on the chronological sequence of excavation.

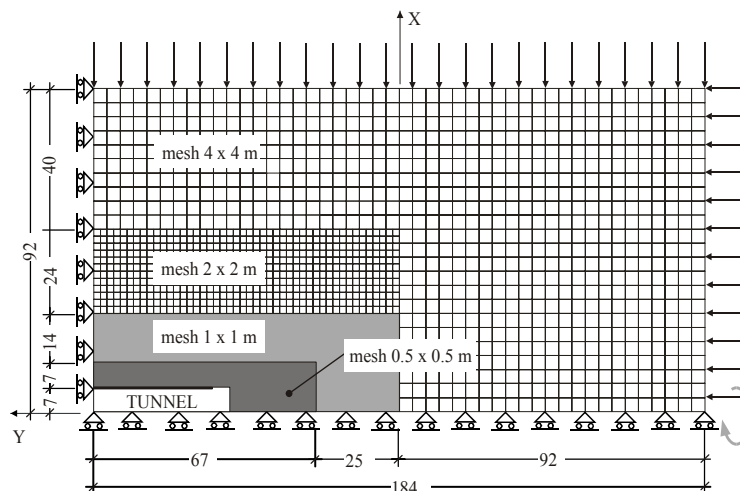


Figure 28. Detail of the FDM grid used for axisymmetric modelling of the tunnel response with SHELVIP.



As for the semi-analytical solution the tunnel is assumed to be circular with an equivalent radius of 5.5 m. The tunnel cross section considered is at chainage 1311 m where the initial isotropic stress is assumed to be 8.4 MPa. As shown in Figure 29, particular attention was posed in describing the excavation sequence versus time; 245 computation steps were needed. The constitutive parameters obtained are given in Table 4. Figures 30 and 31 compare computed and measured radial displacements at the tunnel perimeter (Figure 30) and in the surrounding rock mass (Figure 31). The agreement of the numerical results with the observed values, independent of the scattering of the data derived from performance monitoring in the highly heterogeneous rock mass encountered, is excellent.

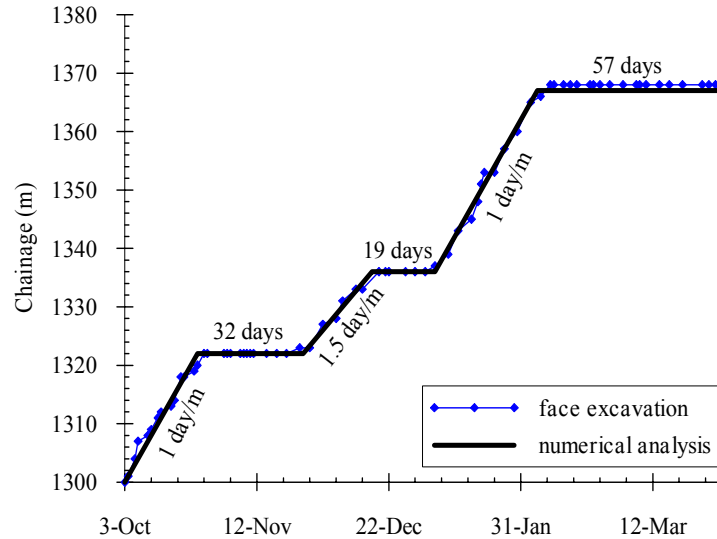


Figure 29. Adopted chronological excavation sequence in the numerical model of P7.3 support system with SHELVIP.

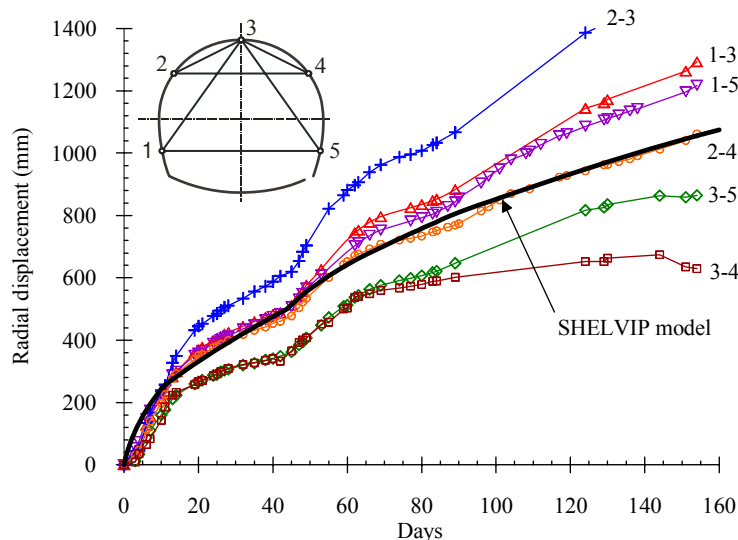


Figure 30. Computed (SHELVIP model) versus monitored radial displacements at chainage 1311 m (P7.3).

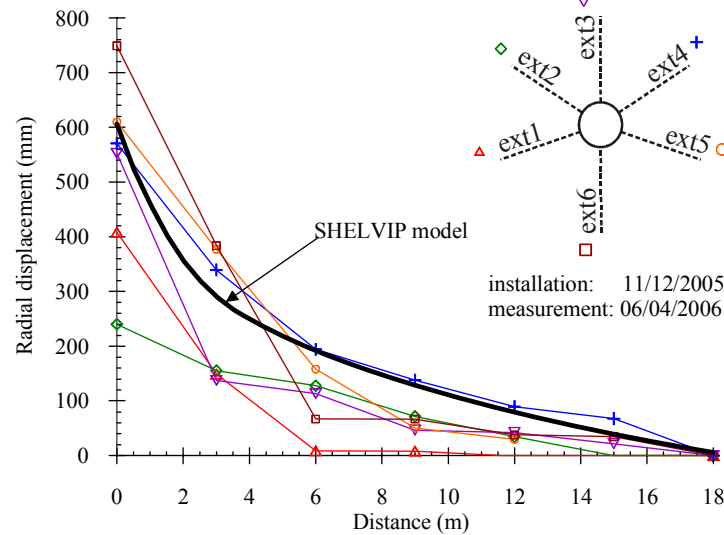


Figure 31. Computed (SHELVIP model) versus monitored radial displacements from multi-position borehole extensometers at chainage 1330 m (P7.3).

Table 4. Constitutive parameters (SHELVIP model) ((*) time in day and pressure in kPa).

Section 1311 m (P7.3)			Section 1443 m (DSM)		
Young's modulus, E	600	MPa	Young's modulus, E	600	MPa
Poisson's ratio, ν	0.3	-	Poisson's ratio, ν	0.3	-
Strength slope, α_p	1.03	-	Strength slope, α_p	1.03	-
Strength intercept, k_p	0.92	MPa	Strength intercept, k_p	0.92	MPa
Tensile strength, σ_t	0.10	MPa	Tensile strength, σ_t	0.10	MPa
Plastic dilatancy, ω_p	0	-	Plastic dilatancy, ω_p	0	-
Fluidity parameter, γ	8.0E-5	(*)	Fluidity parameter, γ	5.1E-5	(*)
Shape factor, m	2,2	(*)	Shape factor, m	2,2	(*)
Load dependency, n	0.18	(*)	Load dependency, n	0.18	(*)
Time factor, l	0.01	(*)	Time factor, l	0.01	(*)
Viscoplastic dilatancy, ω_{vp}	0.735	-	Viscoplastic dilatancy, ω_{vp}	0.735	-

Support System DSM

The tunnel cross section considered, at chainage 1444 m, is again assumed to be circular, with an equivalent radius of 6.0 m. The initial isotropic stress is now 9.8 MPa. As for the previous case, particular attention was posed on a detailed description of the excavation sequence versus time. As shown in Figure 32, an equivalent pressure of 0.1 MPa was applied to the tunnel face in order to account for the reinforcement of the core.

Also simulated, by applying an equivalent radial pressure with the distribution shown in Figure 32, were the tunnel reinforcement and the first-stage lining. The influence of the second-stage lining was introduced with an internal pressure reaching 0.383 MPa in a 5 m span, 30 m behind the face. This value was calculated based on the yielding stress of the deformable elements as determined in the laboratory tests (Figure 11). A constant excavation rate of 0.54 m/day was considered.

The constitutive parameters obtained are given in Table 4. Figures 33 and 34 compare computed and measured radial displacements at the tunnel perimeter (Figure 33) and in the surrounding rock mass (Figure 34). The agreement of the numerical results with the observed values is again satisfactory notwithstanding the already noted scattering of the performance monitoring data due to the high heterogeneity and anisotropy of the rock mass.

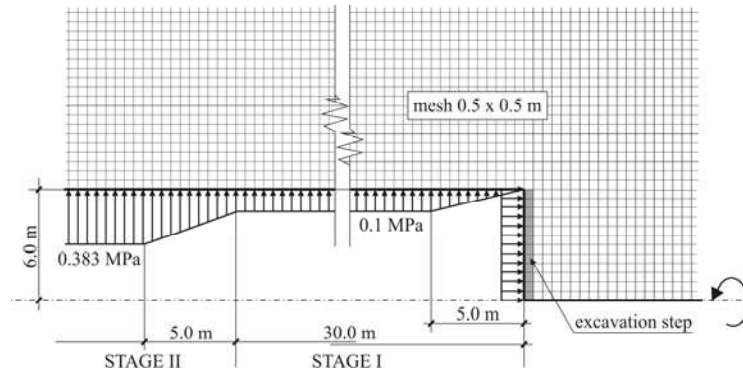


Figure 32. Sketch of the numerical model for the sequence of excavation and reinforcement of DSM support system with the SHELVIP model.

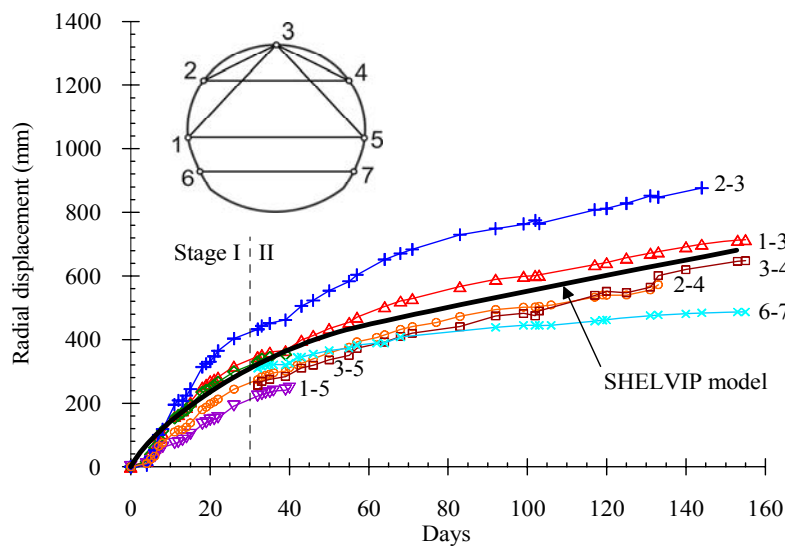


Figure 33. Computed (SHELVIP model) versus monitored radial displacements at chainage 1443 m (DSM).

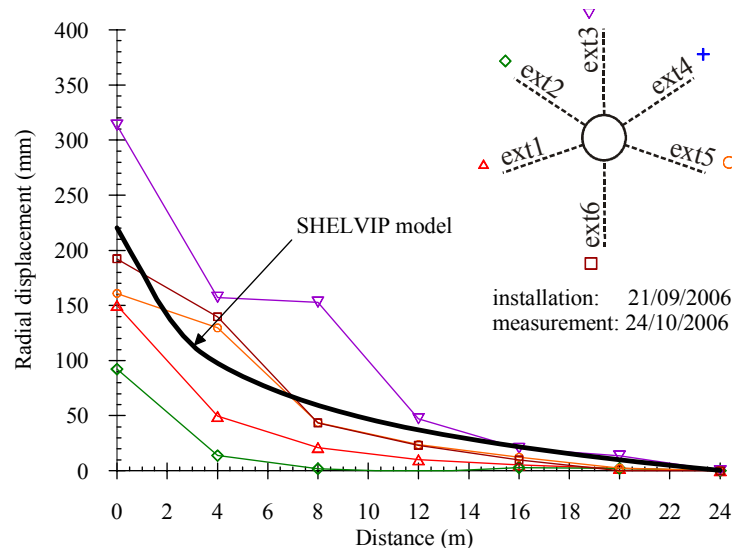


Figure 34(A). Stage I: Computed (SHELVIP model) versus monitored radial displacements from multi-position borehole extensometers at chainage 1443 m (DSM).

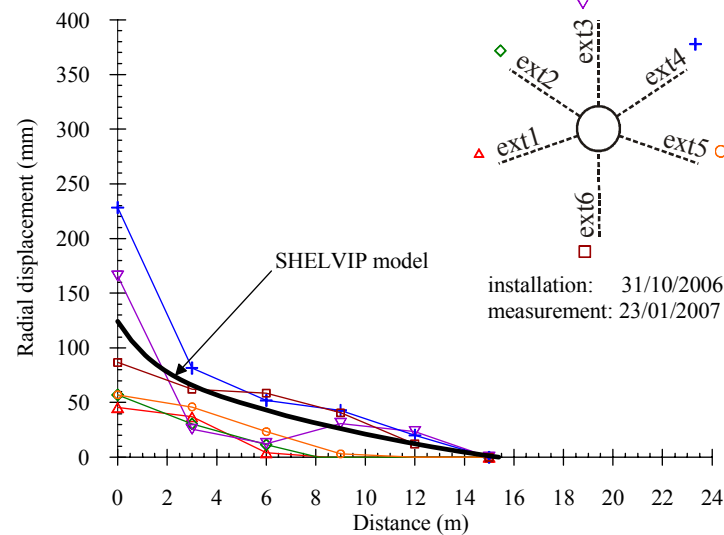


Figure 34(B). Stage II: Computed (SHELVIP model) versus monitored radial displacements from multi-position borehole extensometers at chainage 1443 m (DSM).

CONCLUSIONS

Three constitutive models (CVISC, VIPLA, SHELVIP), each one with different degrees of complexity for representing the time dependent behaviour of the rock mass, were discussed. Among them, of particular interest is the newly developed Stress Hardening ELastic Viscous Plastic model (SHELVIP), which was shown to describe, with acceptable level of confidence, the main features of behaviour observed during excavation of large size tunnels which exhibit severe to very severe squeezing conditions.

The SHELVIP model was derived from the Perzyna's overstress theory, by adding a time independent plastic component. According to the classical theory of elastoplasticity, the time-independent plastic strains develop only when the stress point reaches the plastic yield surface defined by the Drucker-Prager criterion. The viscoplastic strain rates develop only if the effective stress state exceeds a viscoplastic yield surface which is also defined by the Drucker-Prager criterion.

An innovative excavation-construction method with the use of yielding support elements incorporated in the primary lining was described. This was implemented in order to cope with the very severe to severe squeezing problems encountered during excavation of the Saint Martin La Porte access adit, along the Lyon-Turin Base Tunnel, in a Carboniferous Formation, a highly heterogeneous, disrupted and fractured rock mass, often affected by faulting.

The tunnel response which was continuously monitored during face advance was analysed in detail. As an illustration of the application of the VIPLA model a semi-analytical solution was used. Numerical modelling by the Finite Difference Method was applied in conjunction with the CVISC and the SHELVIP models, in plane strain and axisymmetric conditions respectively. In all cases the computed and monitored deformations around the tunnel during face advance were compared, showing the advantages and disadvantages of each model in describing the complex deformational response being observed during excavation.

It is shown that when the CVISC model simulates the tunnel "short term" response, at the end of stage 1 (23 days after excavation) the convergence along array 1-5, namely 314 mm, is close to the in situ value (336 mm). As expected, the model does not predict the observed deformation thereafter, when the tunnel exhibits a gradual decrease in the rate of convergence, reaching a near stable condition. This is essentially due to the rather simple mathematical formulation of the CVISC model.

The results obtained for both the P7.3 and DSM sections highlight that the VIPLA model reproduces the time dependent tunnel response more satisfactorily than the CVISC model, also considering that a semi-analytical solution for a circular tunnel was used. The main limitation of the VIPLA model is found in the absence of a true plastic limit that cannot be



exceeded by the effective state of stress in the rock mass. This is not a very significant drawback as long as one is to describe the time dependent deformations around the tunnel.

With the intent to overcome the limitations of the CVISC and VIPLA constitutive laws in modelling the tunnel response as outlined above, the newly developed SHELVIP model (Debernardi and Barla, 2009; Debernardi, 2008) was adopted. In this case the agreement of the numerical results with the observed values is shown to be with acceptable level of confidence satisfactory for the duration of the in situ monitoring, notwithstanding the already noted scattering of the data due to the high heterogeneity and anisotropy of the rock mass. The authors are aware that the modelling provided in this paper can be improved to account for such aspects as the three-dimensional conditions at the tunnel face and by introducing a more detailed representation of the support system being used.

REFERENCES

- Barla, G. (2005). "Design analyses for tunnels in squeezing rock". Proc. 11th International Conference of IACMAG, Torino, Italy, 3-22.
- Barla, G., Bonini, M., and Debernardi, D. (2007). "Modelling of tunnels in squeezing rock". Proc. ECCOMAS Thematic Conference on Computational Methods in Tunnelling (EURO:TUN 2007), Vienna, Austria. Eberhardsteiner et al. (eds.). Vienna University of Technology, Austria.
- Barla, G., Debernardi, D., and Sterpi, D. (2009) "Numerical analysis of tunnel response during excavation in squeezing rock by using two constitutive models". EURO:TUN 2009 2nd International Conference on Computational Methods in Tunnelling. Ruhr University, Bochum, Germany.
- Debernardi, D. (2008). "Viscoplastic behaviour and design of tunnels". PhD Thesis, Politecnico di Torino, Department of Structural and Geotechnical Engineering, Italy.
- Debernardi, D., and Barla, G. (2009), "New Viscoplastic Model for Design Analysis of Tunnels in Squeezing Conditions". Rock Mech. Rock Engng., 42(2), 259-288.
- GDP Consultants Engineering Geology (2009). Descenderie De Saint Martin La Porte - Profil Geologique.
- Hoek, H. (2001). "Big tunnels in bad rock". ASCE Journal of Geotechnical and Geoenvironmental Engineering, 127(9), 726-740.
- Itasca (2006). Flac2D 5.0, User's Manual. Minneapolis, USA.
- Lagarias, J.C., Reeds, J.A., Wright, M.H., and Wright, P.E. (1998). Convergence Properties of the Nelder-Mead Simplex Method in Low Dimensions. SIAM J. Optim. 9, 112-147.
- Lemaitre, J. and Chaboche, J.L. (1996). Mécanique des matériaux solides. Dunod, 253-341.
- Martinotti, G. (2009). Expertise géologique et hydrogéologique dans les secteurs des descenderies de La Praz – St Martin la Porte. Partie géologie St Martin la Porte.
- Nguyen-Minh, D. and Pouya, A. (1992). "Une méthode d'étude des excavations souterraines en milieu viscoplastique". Revue Française de Géotechnique 59, 5-14.
- Panet, M. (1995). Le calcul des tunnels par la méthode convergence-confinement. Presse de l'école des Ponts et chaussées, Paris.
- Perzyna, P. (1966). "Fundamental Problems in Viscoplasticity". Advances in Applied Mechanics, Academic Press 9, 243-377.



INTERNATIONAL JOURNAL OF
**GEOENGINEERING
CASE HISTORIES**

*The Journal's Open Access Mission is
generously supported by the following Organizations:*



Access the content of the *ISSMGE International Journal of Geoengineering Case Histories* at:
www.geocasehistoriesjournal.org